Theoretical and Applied Climatology (2025) 156:104
https://doi.org/10.1007/s00704-024-05348-0

RESEARCH

Quantifying the role of vegetation on urban heat over Bengaluru, India

Heather S. Sussman[1,2] · Aiguo Dai[2] · Liming Zhou[2]

Received: 2 July 2024 / Accepted: 27 December 2024

Abstract
The urban heat island (UHI) effect refers to how cities tend to be warmer than their non-urban surroundings, which increases the risk for heat-related illnesses and amplifies energy demands. Therefore, developing UHI mitigation strategies is crucial. Bengaluru, India has been rapidly urbanizing, but has yet to receive attention regarding potential UHI mitigation strategies. This work uses the Weather Research and Forecasting model with the single-layer urban canopy model to determine how UHI intensity changes in Bengaluru with perturbations of −10%, +10%, +20%, and +30% in vegetation amount since recent work has shown that vegetation amount is the leading control of urban heat in Bengaluru. These perturbations illustrate how much the UHI could be amplified by near-depletion of vegetation or mitigated via realistic increases in vegetation. The simulations were investigated diurnally and during the dry and wet seasons. Results show that increases in vegetation were associated with a decrease in urban land surface temperature, an increase in the latent heat flux, and decreases in the sensible heat flux, and vice versa for a decrease in vegetation. Significant changes in UHI intensity usually occurred only when vegetation was increased by 20% or more. However, for the dry season nighttime, which exhibited the highest UHI intensity in the control run (1.70ºC), the 10% increase in vegetation produced a significant decrease of −0.19ºC in UHI intensity, likely due to a shallow planetary boundary layer height. These results could have implications for mitigating urban heat, and reducing energy demands and public health risk in Bengaluru.

Keywords Bengaluru · Urban canopy model (UCM) · Urban heat island (UHI) · Vegetation · Weather research and forecasting (WRF) model

1 Introduction

Urbanization can have many positive socioeconomic impacts, such as the creation of jobs and commerce hubs. However, urbanization can also deteriorate the environment that half the world calls home (Grimm et al. 2008). Urban areas tend to have poor air quality due to manufacturing and vehicular traffic (Ramachandran et al. 2012), which can increase the risk for respiratory illnesses (Filho et al. 2018). Cities can also modify regional climate. For example, Kishtawal et al. (2010) noted an increase in the frequency of heavy precipitation episodes during the monsoon season over Indian cities with increased urbanization. Regional climate modifications could have impacts on an area's economy. For instance, India's agricultural sector depends on the proper amount of monsoon rainfall each year (Parthasarathy 1984).

A common urbanization impact is the tendency of urban areas to be warmer than their nearby non-urban surroundings, i.e., the urban heat island (UHI) phenomenon (Oke 1982). In a warming climate, the UHI effect is of particular importance due to the increased risk of heat exhaustion and higher energy demands for cooling (Filho et al. 2018). The UHI effect results from the contrast between urban and non-urban surface properties. Urban surfaces are characterized by low vegetation cover and low albedo due to paved dark surfaces, which increases the amount of absorbed solar radiation and reduces evaporative cooling via decreases in

✉ Heather S. Sussman
Heather.S.Sussman@usace.army.mil

[1] U.S. Army Engineer Research and Development Center – Geospatial Research Laboratory, 7701 Telegraph Rd., Alexandria, VA 22315, USA

[2] Department of Atmospheric and Environmental Sciences, University at Albany, State University of New York, 1400 Washington Ave, Albany, NY 12222, USA

Published online: 15 January 2025

the latent heat (LH) flux, and subsequent increases in the sensible heat (SH) flux and Bowen ratio. These surface flux changes cause the urban surface to warm quickly during the daytime, which increases heat storage and the ground heat (GH) flux during the day and enables the surface to retain more heat at nighttime through a slow heat release (Taha 1997). In contrast, non-urban surfaces typically have higher vegetation cover, albedo, and heat release, which promotes evaporative cooling and the reflection of solar radiation. Therefore, warmer surface and 2-m temperatures often exist for a city compared to its non-urban surroundings. The strength of a city's UHI is often termed the UHI intensity, i.e., the mean urban surface temperature minus the mean non-urban surface temperature, which can be influenced by season, time of day, surface conditions, meteorological conditions, and building materials.

It is worthwhile to develop UHI mitigation strategies to potentially curb the risk of heat and respiratory illnesses for urban inhabitants and visitors. Chen et al. (2011) noted that the Weather Research and Forecasting (WRF) model can simulate the UHI phenomenon due to its development of urban parameterization schemes, i.e., urban canopy models (UCMs). Therefore, WRF is widely used to study issues related to the urban environment, including mitigation strategies, for cities across the world. However, thus far such studies have mainly focused on cities in North America, Europe, and East Asia. Different mitigation strategies have been tested, such as the use of increasing vegetation and/or albedo of building roofs, i.e., green and cool roofs (e.g., Li and Norford 2016; Imran et al. 2018). Other studies have increased vegetation of city surfaces that were vacant, such as abandoned parking lots (Cady et al. 2020), or increased vegetation cover by a certain percentage throughout the urban area (Beradi et al. 2020).

Overall, there are numerous mitigation approaches that could potentially reduce UHI intensity, and some approaches may work better for certain cities. To evaluate UHI mitigation strategies for a given city, mitigation methods should be based on the leading mechanisms of the UHI formation for that city. Several studies have used statistical and machine learning methods to determine the relative importance of variables such as vegetation, albedo, aerosols, etc., in influencing urban heat for various cities, as these results are often city specific (e.g., Kim and Baik 2002; Zhou et al. 2011; Lokoshchenko and Alekseeva 2023; Xu et al. 2024). This information is crucial so that mitigation strategies are mechanism-based and city-specific, and thereby directly target the main drivers of the UHI (Lenzhöler and Van der Wulp, 2010).

Over India, studies addressing UHI mitigation are lacking, despite India having the world's second largest population with many metropolises (United Nations 2018) and numerous observational studies on UHI characteristics throughout the country (Veena et al. 2020). Therefore, the need exists to evaluate mechanism-based mitigation strategies for cities in India. The city of Bengaluru, which is centrally located in southern India (city center: 12.97°N, 77.59°E) on the Deccan Plateau at an elevation of 900 m, is the third most populous city in India with a population of ~13 million. Interestingly, Bengaluru was once known as the *"Garden City"* of India, but now as the *"Silicon City"* due to the increased presence of the information technology industry (Sudhira et al. 2007). Recently, Sussman et al. (2021) used multiple linear regression and the random forest to determine the relative importance of several environmental variables in controlling urban land surface temperature (LST) in Bengaluru. They found both statistical models to suggest vegetation amount as the leading controlling factor of urban heat in Bengaluru for the dry season (December-January-February; DJF) daytime and nighttime and for the wet season (August-September-October; ASO) daytime. For ASO nighttime, they found specific humidity to be the leading controlling factor, which was positively correlated to vegetation amount. Therefore, urban heat is primarily controlled by vegetation in Bengaluru. As a result, UHI mitigation strategies for Bengaluru should involve methods to increase vegetation.

Given that previous studies have not used WRF to quantify the role of vegetation on UHI intensity in India and that vegetation is the leading controlling factor of urban heat in Bengaluru, this work strives to answer the following questions diurnally for both DJF and ASO:

1) What are the LST, LH, SH, and GH responses to varying perturbations of vegetation over Bengaluru?
2) How strong are the relationships between the change in LST and changes in the LH, SH, and GH fluxes?
3) Can the UHI of Bengaluru become neutral only by a vegetation increase of a realistic amount?

2 Methods

2.1 Numerical simulations

WRFv4.2.2 (Skamarock et al. 2019) was used to perturb vegetation over Bengaluru and investigate the simulated responses in LST, the LH, SH, and GH fluxes, and UHI intensity as compared to a reference case. The model setup is based on the conclusions of Sussman et al. (2024), who conducted WRF simulations to assess model performance in simulating LST over Bengaluru and the sensitivities to UCM and planetary boundary layer (PBL) scheme choices. The reader is referred to Sussman et al. (2024) for full

details about how UCMs work and all results of the model evaluation, including the specific biases. The key points of the model evaluation and model setup are explained below.

All simulations were run for 61 days, in which the first 24 h was used as the spin-up period. The DJF simulations were run from 00 UTC on 16 December 2017 through 14 February 2018 and the ASO simulations were run from 00 UTC on 16 August 2018 through 15 October 2018. These simulations were performed for 2018 since it is most representative of current conditions and to be consistent with Sussman et al. (2019, 2021) who analyzed the characteristics and controls of Bengaluru's UHI for 2003–2018. As done by Sussman et al. (2024), the daytime analysis for this study was performed by averaging all variables using the 05:00 and 08:00 UTC output (i.e., 10:30 and 13:30 Indian Standard Time or IST) and the nighttime analysis was done by averaging the 17:00 and 20:00 UTC output (22:30 and 01:30 IST). These sampling times were chosen since they coincide as best as possible to the diurnal timing of the averaged observations from Moderate Resolution Imaging Spectroradiometer (MODIS) LST data, which was used to evaluate WRF (Sussman et al. 2024).

The physical parameterizations used for all simulations included Dudhia shortwave radiation (Dudhia 1989), the rapid radiative transfer model (RRTM) for longwave radiation (Mlawer et al. 1997), Thompson microphysics (Thompson et al. 2008), the Eta similarity scheme for the surface layer (Janjić 1994), the Bougeault and Lacarrerè (BouLac) PBL scheme (Bougeault and Lacarrerè 1989), the single-layer UCM (SLCUM; Kusaka et al. 2001) and the Noah Land Surface model (Chen and Dudhia 2001). Sussman et al. (2024) found that for DJF and ASO daytime and nighttime, three out of these four cases had the SLUCM as the best performing UCM and three out of these four cases had BouLac as the best performing PBL scheme in simulating urban LST and UHI intensity over Bengaluru. Therefore, the SLUCM and BouLac were chosen for all simulations in this study to have consistent physics, including the reference control (CTL) run.

All simulations were forced by hourly ERA5 reanalysis data on 0.25º grids (Hersbach et al. 2020) and ran with a 6 s timestep. Spectral nudging was used to ensure the WRF-simulated fields follow the large-scale variations in the forcing data in the free troposphere (Liu et al. 2017). Each simulation had 42 vertical levels with the top at 50 hPa and 11 levels below 2 km to better resolve the PBL. All simulations were performed over a single domain of 150 km × 150 km with 1 km grid spacing focused on the Bengaluru city center (Fig. 1). Therefore, no cumulus parameterization was used due to the convective-permitting grid spacing for the domain (Liu et al. 2017).

Each simulation had its land cover defined using MODIS Aqua and Terra combined annual-mean land cover from Collection 6 (MCD12Q2) for 2018 on 1 km grids as shown in Fig. 1. MODIS defines land cover type as the dominant land cover within each grid and according to the classifications developed by the International Geosphere-Biosphere Programme (IGBP). The IGBP defines urban land cover as grids that have at least 30% of its surface area as impervious (Belward et al. 1999). In this manner, WRF assigns each grid 100% of the dominant land cover type shown in Fig. 1. However, each grid may not be composed entirely of the specified land cover type. To alleviate this issue, when using an UCM, the parameter urban fraction (FRC_URB2D) allows the user to specify the fraction of impervious surface in the WRF urban grids to represent various degrees of development, i.e., 0.95 represents commercial/industrial development, 0.90 represents high-density residential, and 0.50 represents low-density residential (Chen et al. 2011). While these broad categories exist, any value between 0 and 1 can be chosen for urban fraction. In the CTL runs, urban fraction was set to 0.90 for all urban grids (Sussman et al. 2024). Therefore, for each urban grid in the CTL runs, the sub-grid is parameterized as 90% impervious, urban land and 10% pervious, vegetated land (Chen et al. 2011). A value of 0.90 was chosen since the MODIS enhanced vegetation index (EVI) dataset showed that Bengaluru has urban greenness values ranging between 0.05 and 0.25 in DJF and ASO, with majority of the urban grids having EVI values closer to the lower limit (Sussman et al. 2019).

To perturb vegetation, urban fraction was altered. Four perturbations to urban fraction were made relative to the CTL value of 0.90 for all urban grids: (1) a browning or continued urbanization scenario (URB) in which urban fraction was increased by 10% to 0.99, (2) a conservative greening scenario (CON) in which urban fraction was decreased by 10% to 0.81, (3) a moderate greening scenario (MOD) in which urban fraction was decreased by 20% to 0.72, and (4) an aggressive greening scenario (AGR) in which urban fraction was decreased by 30% to 0.63 (Table 1). In this way, the fraction of pervious, vegetated area (i.e., 1–FRC_URB2D) of each urban grid is 0.01 in URB, 0.19 in CON, 0.28 in MOD, and 0.37 in AGR. This approach is similar to Cady et al. (2020), but with the added perturbation of increasing urban fraction (i.e., the URB experiment) to understand how UHI intensity could increase if urbanization continues without any mitigation efforts and if near-depletion of vegetation over the city occurs. By performing four perturbation experiments and including the CTL from Sussman et al. (2024), a 5-member ensemble of urban fraction scenarios will be developed, which can be used to estimate changes to LST at other urban fraction values. These perturbation experiments

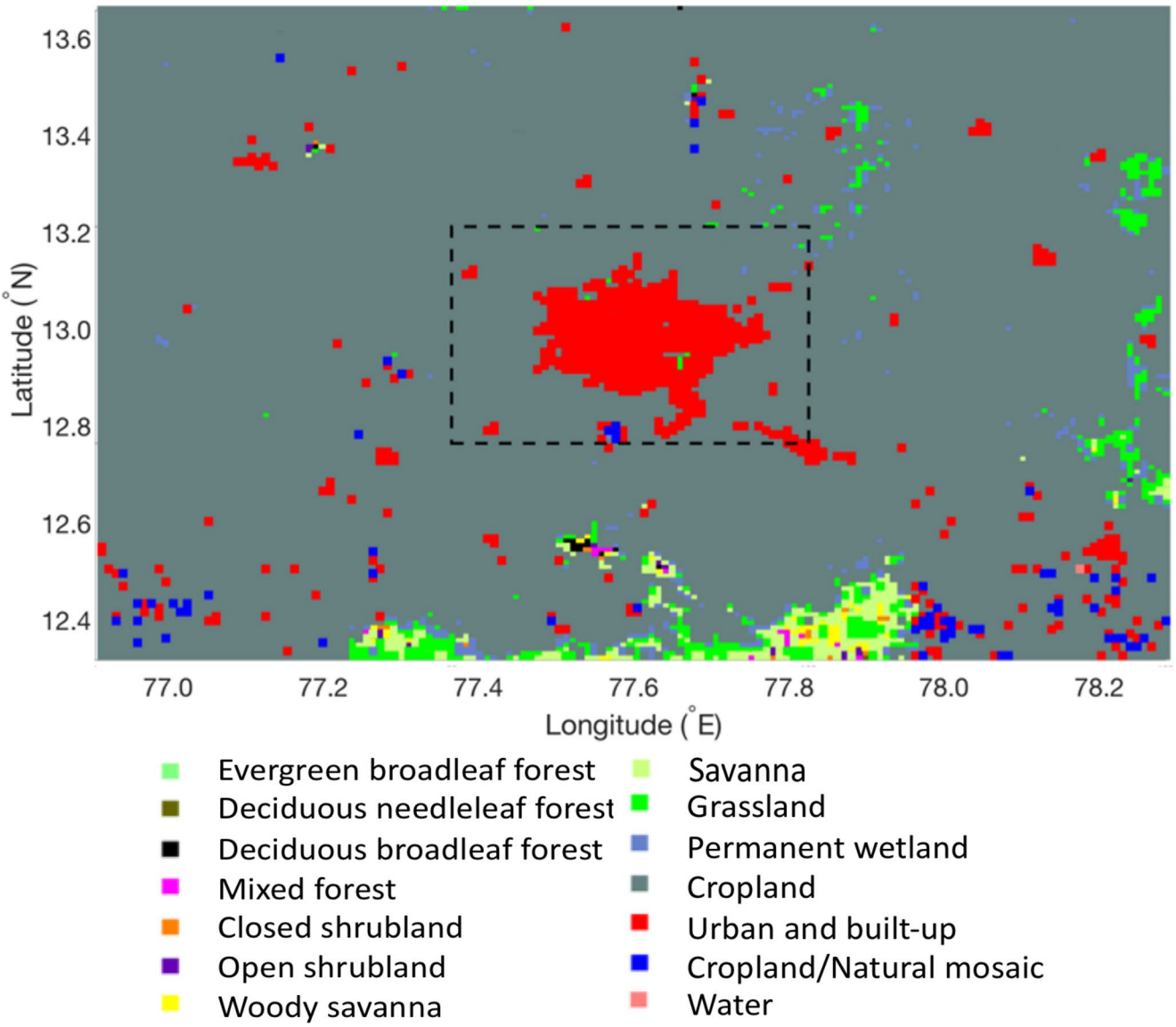

Fig. 1 The 150 km × 150 km domain with 1 km grid spacing used for all WRF simulations. The background shows the 2018 land cover distribution specified by MODIS, i.e., the land cover used in all simulations. The black dashed square represents the 50 km × 50 km area used for all analyses. In the WRF simulations, the urban grids are not 100% urban in the sub-grid scale due to the use of the SLUCM, which enables the urban fraction parameter to be used

Table 1 The urban fraction (FRC_URB2D) values used in the control (CTL), continued urbanization (URB), conservative greening (CON), moderate greening (MOD), and aggressive greening (AGR) simulations for all urban grids. The 1–FRC_URB2D represents the pervious, vegetation fraction in the sub-grid scale of each urban grid

Experiment	FRC_URB2D	1–FRC_URB2D
CTL	0.90	0.10
URB	0.99	0.01
CON	0.81	0.19
MOD	0.72	0.28
AGR	0.63	0.37

were done for DJF and ASO, thus eight WRF simulations were performed for this study.

Changes to urban fraction also influence other land surface variables. For example, as urban fraction decreases and more pervious, vegetated land cover is parameterized in the urban grids, the urban albedo increases. An increase in surface albedo decreases the amount of absorbed shortwave radiation over the city, which could contribute to a decrease in urban LST and consequentially UHI intensity. However, the albedo over the urban surface in the perturbation experiments never became as high as that of the non-urban surroundings. Overall, the albedo changes were small and of less than a 5% increase from the CTL to AGR simulations.

Investigating these indirect changes due to perturbations of urban fraction are beyond the scope of this study as these changes are likely included in the LST and UHI intensity changes.

2.2 Analysis

All analyses were carried out over the central 50 km × 50 km region of the WRF domain (Fig. 1), which is the same area analyzed in Sussman et al. (2019, 2021, 2024). For each simulation, the mean change relative to CTL over the 50 km × 50 km area in LST, LH, SH, and GH was computed. The mean change in LST, LH, SH, and GH was then averaged only over the model urban grids (Fig. 1). In an attempt to have each urban grid be in its "purest" form, if an urban grid was 2 km or less away from a cropland (i.e., non-urban) or water grid, it was excluded from the urban averaging in an effort to reduce possible contamination of cooler LST, higher LH fluxes, and lower SH and GH fluxes from the nearby vegetated and water areas (Sussman et al. 2024). To determine how strong the relationships are between the urban LST response and changes in the urban LH, SH, and GH fluxes, the linear temporal correlation coefficient and slope was computed for the urban LST change with both the urban LH, SH, and GH change, relative to the CTL for each experiment and for day and night. The simulation mean urban LST, LH, SH, and GH were also computed. The slope among the four simulation means was computed to assess how changes in vegetation influence the seasonal-mean of the variables. For these analyses, the LH flux was assessed only during daytime since the LH flux is mainly driven by solar radiation with near-zero values during nighttime, regardless of vegetation amount.

The mean UHI intensity and its mean change relative to the CTL were computed for each simulation. UHI intensity was computed as the mean urban LST minus the mean non-urban LST. The non-urban LST was computed using the cropland grids (Fig. 1). Grids are classified as cropland by MODIS, and subsequentially by WRF, if at least 60% of the grid is cultivated cropland in which the lands are covered by temporary crops followed by a harvest and a bare soil period (e.g., single and multiple cropping systems), according to the IGBP (Belward et al. 1999). Similar to the computation of urban LST, efforts to have the non-urban LST be in its "purest" form were accomplished by excluding a non-urban (i.e., cropland) grid in the calculation if it was 2 km or less away from an urban or water grid (Sussman et al. 2024). The linear line of best fit was then computed for the numerical relationship between urban fraction and mean UHI intensity. Using this equation, the urban fraction needed to achieve a 0°C UHI intensity was determined to understand if a neutral UHI can be obtained by solely increasing vegetation over Bengaluru by a uniform amount. Statistical significance of all the above analyses was assessed using the two-tailed Student's t-test with a p-value ≤ 0.10 considered to be statistically significant.

3 Results and discussion

3.1 Vegetation-induced changes in LST, LH, SH, and GH

Figure 2 shows the mean change patterns in LST, LH, SH, and GH for DJF daytime from all experiments as compared to the CTL. Overall, results are as expected. Decreasing the vegetation fraction from 10 to 1% for all urban grids in the URB experiment induces a mean increase in LST of 0.22°C, a mean decrease in LH of 33.15 Wm^{-2}, a mean increase in SH of 7.84 Wm^{-2}, and a mean decrease in GH of 17.35 Wm^{-2} over the urban area. These results indicate less evaporative cooling, more thermal heating of the air, and more ground heat storage since all fluxes are positive upward. In contrast, increased vegetation in the CON, MOD, and AGR experiments induces a decrease in LST and SH and an increase in LH and GH, with the magnitude of the changes increasing with more vegetation (Fig. 2). Additionally, while differences exist throughout the domain, the dominant change is only over the urban grids where urban fraction was perturbed. As in Cady et al. (2020), the small changes in the non-urban surroundings are associated with the turbulent nature of the lower atmosphere and behave as white noise. For a 10% increase or decrease in urban fraction, the variables change by a similar amount with an opposite sign. For all experiments, the LH magnitude change is about four times that of the SH change and is about two times that of the GH change. The LH change ranges from −233.15 to 99.46 Wm^{-2}, compared to the SH change of 7.84 to −225.04 Wm^{-2} and the GH change of −217.35 to 51.35 Wm^{-2}. This is likely due to changes in vegetation directly impacting surface evapotranspiration, which subsequently changes LST and the SH and GH fluxes (Taha 1997). While the LH, SH, and GH flux changes are significant over most urban grids for all experiments, the LST changes are significant only over some grids in MOD and AGR, and the mean urban LST change is significant only in AGR. This indicates that large changes in the LH, SH, and GH fluxes are needed to cause significant changes in LST over Bengaluru in DJF daytime.

Figure 3 shows the mean change patterns and urban-mean changes in LST, LH, SH and GH for ASO daytime from each experiment. Similar to DJF daytime, decreased vegetation in the URB experiment induces a mean increase in LST of 0.19°C, a mean decrease in LH of 35.08 Wm^{-2},

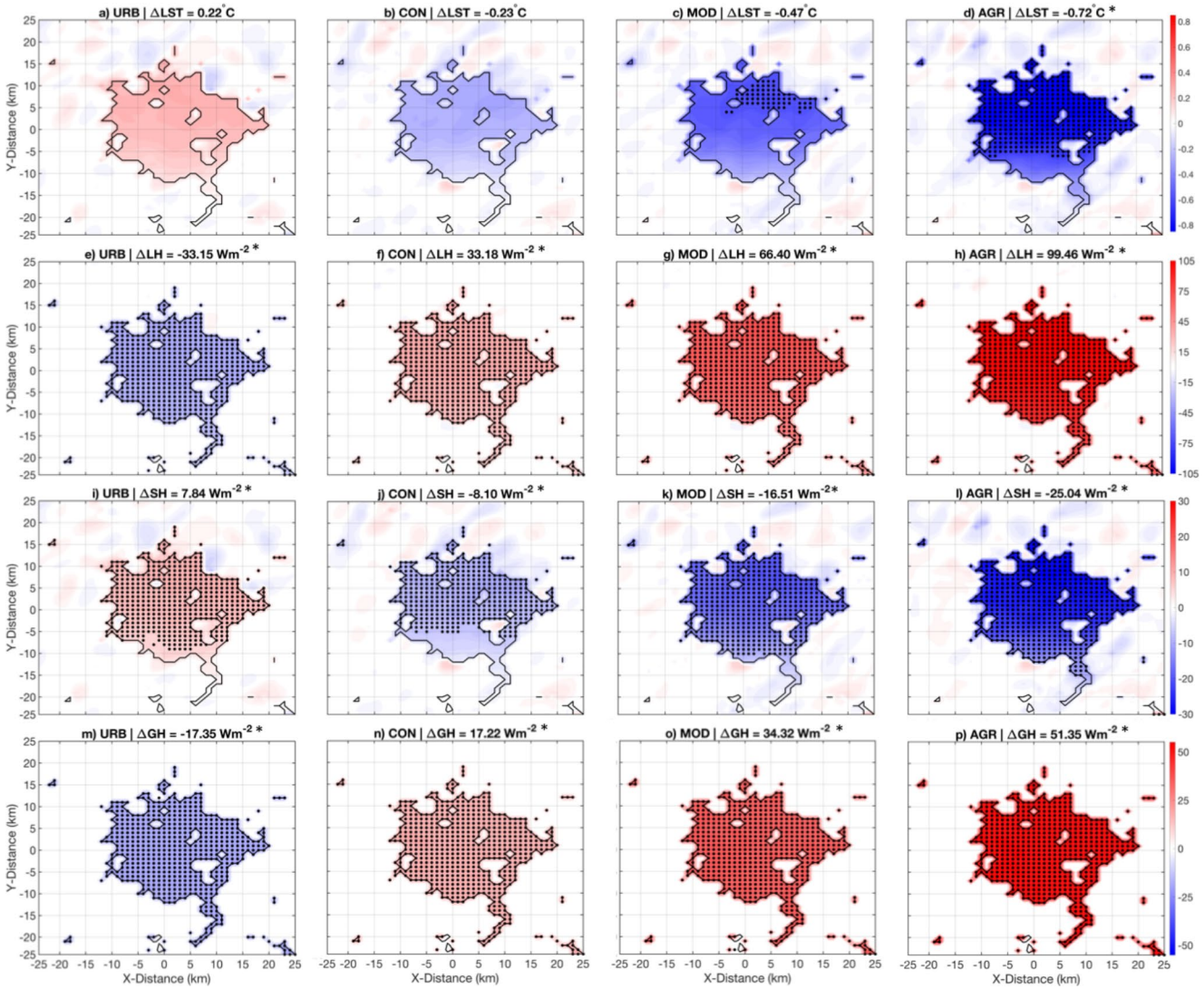

Fig. 2 (**a**–**d**) The 17 December 2017–14 February 2018 (DJF) mean daytime change relative to the CTL simulation in LST (°C) for the URB, CON, MOD, and AGR simulations. Stippling indicates that the mean change is significant at the 10% level based on the two-tailed Student's t-test. The mean change averaged over the urban surface (Δ LST) is shown on top of each panel with an asterisk indicating that the mean change is significant at the 10% level based on the two-tailed Student's t-test. (**e**–**h**) Same as (a–d), but for the LH flux (Wm^{-2}). (**i**–**l**) Same as (**a**–**d**), but for the SH flux (Wm^{-2}). (**m**–**p**) Same as (**a**–**d**), but for the GH flux (Wm^{-2}). All fluxes are positive upward

a mean increase in SH of 7.93 Wm^{-2}, and a mean decrease in GH of 16.72 Wm^{-2} over the urban area. The SH change is comparable to DJF daytime (7.84 Wm^{-2}), but the LH and GH change are slightly more than in DJF daytime (−233.15 Wm^{-2} and −217.35 Wm^{-2}, respectively in DJF daytime). However, the mean LST change is slightly less than in DJF daytime (0.22°C). Also similar to DJF daytime are the small spatial variations in the change patterns, significance of the LH, SH and GH changes over most urban grids for all experiments (except for SH in URB), and the mean urban LST change is significant only in AGR. These results indicate that even larger changes in the LH, SH, and GH fluxes are needed to cause significant changes in LST over Bengaluru in ASO daytime compared to DJF daytime.

Figure 4a–d show the mean spatial change patterns in LST for DJF nighttime. The LST changes are of greater magnitude and are not as linear compared to DJF daytime for each 10% change in urban fraction. The mean urban LST increased by 0.35°C in URB, decreased by 0.39°C in CON, which then decreased by 0.44°C to a mean decrease of −20.83°C in MOD, and decreased further by 0.50°C to a mean decrease of −21.33°C in AGR. Additionally, some weak changes in LST to the west of the city are seen in each simulation, which is most noticeable in the MOD and AGR experiments. During DJF nighttime, the mean simulated wind direction is from the east to the west (not shown). As a result, a downwind LST change appears due to advection. Previous studies have also noted the occurrence of a

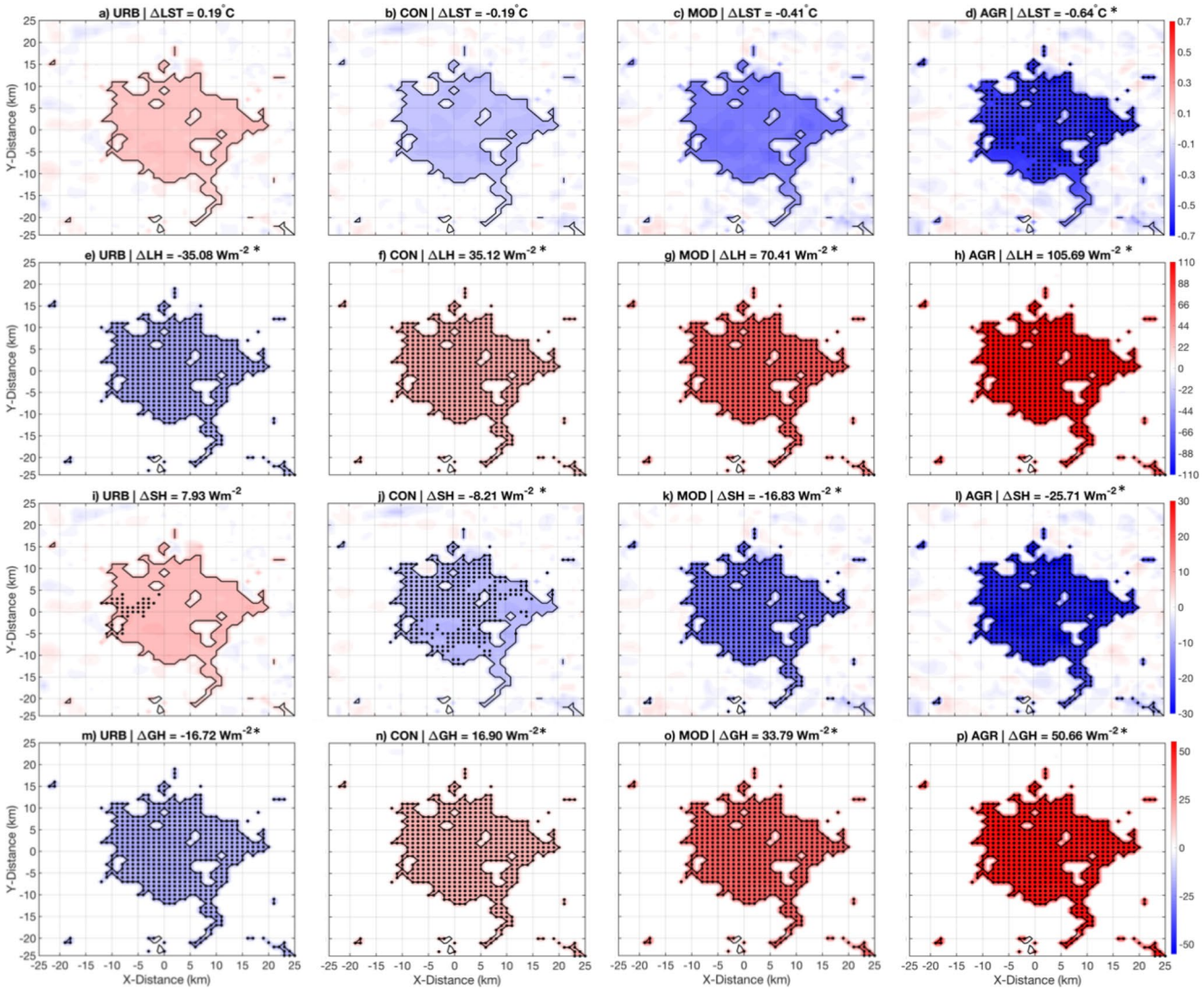

Fig. 3 Same as Fig. 2, but for ASO daytime (i.e., 17 August 2018–15 October 2018)

downwind effect that is mainly observed at nighttime when the boundary layer is not as deep nor well-mixed as in daytime (e.g., Cady et al. 2020). The WRF simulated mean PBL height over the urban grids in Bengaluru for all simulations is highest for ASO daytime, followed by DJF daytime, ASO nighttime, and lastly DJF nighttime (Table 2). The mean PBL height is highest in ASO daytime due to higher solar heating and LST. The mean PBL height does not exhibit large changes during daytime across the simulations but has larger decreases with more vegetation during nighttime as surface roughness, urbanization intensity, and surface heating all decrease (Table 2).

The SH change patterns in DJF nighttime (Fig. 4e–h) are similar to DJF and ASO daytime for each experiment. However, the magnitude of the change is smaller. Here, a 10% change in urban fraction causes approximately a 4 Wm^{-2} mean change in SH. Related to the downwind effect, the area west of the city exhibits a small decrease in the SH flux for the URB experiment and an increase in the SH flux for the CON, MOD, and AGR experiments that becomes higher in magnitude with a higher increase in vegetation. A few grids show significant differences in SH for the AGR experiment. The local SH flux is mainly dependent on the local wind speed and difference between LST and 2-m temperature, in that a higher difference causes more vertical turbulent heat transfer, and thus a higher SH flux. For the CON, MOD, and AGR experiments, advection cooled 2-m temperature more than LST to the west of the city, which led to an increased LST and 2-m temperature difference downwind, with the largest difference occurring for the AGR experiment (not shown). Consequentially, the SH flux increased to the west of the city, and since the increase is largest in AGR, some grids were significant. The opposite occurs for URB as advection warms 2-m temperature more than LST causing a

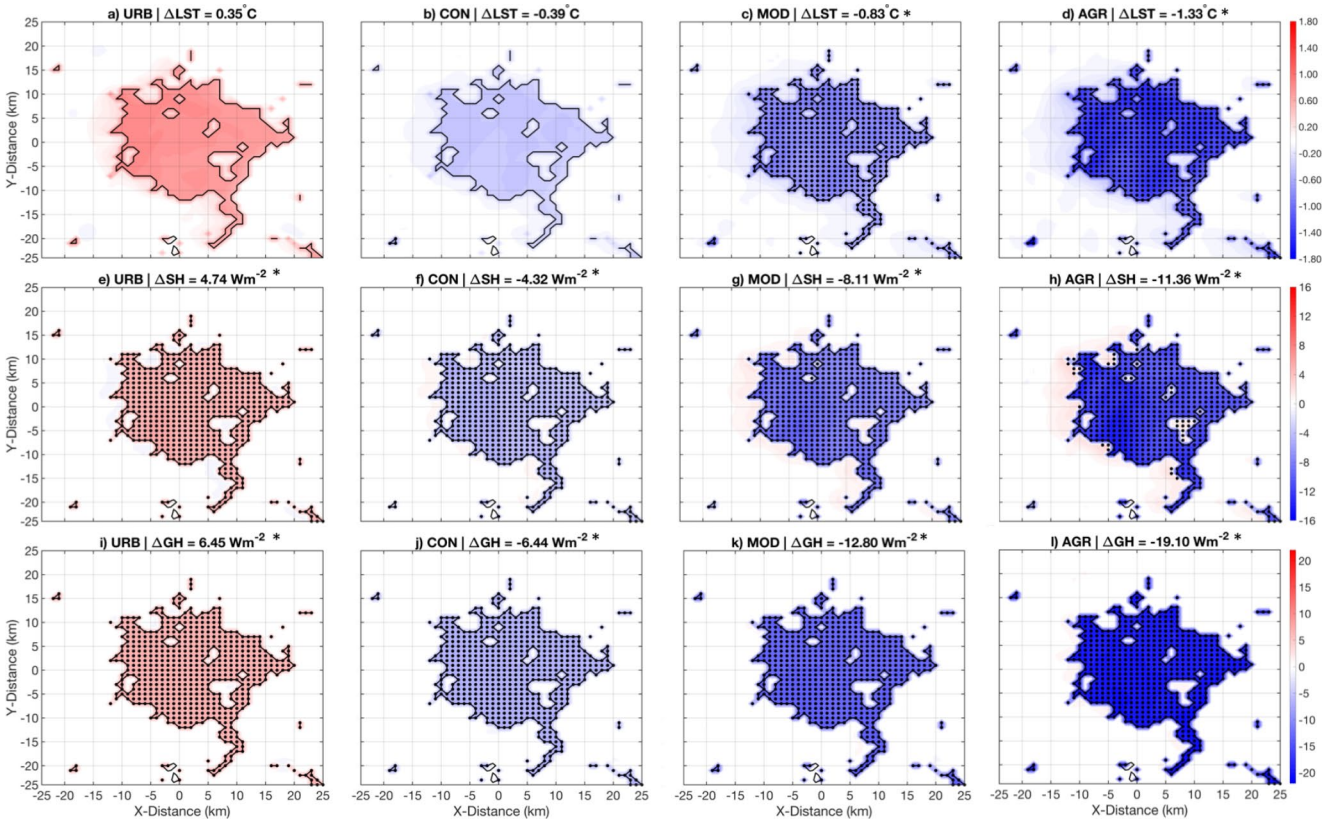

Fig. 4 (**a**–**d**) The 17 December 2017–14 February 2018 (DJF) mean nighttime change relative to the CTL simulation in LST (°C) for the URB, CON, MOD, and AGR simulations. Stippling indicates that the mean change is significant at the 10% level based on the two-tailed Student's t-test. The mean change averaged over the urban surface (Δ LST) is shown on top of each panel, with an asterisk indicating that the mean change is significant at the 10% level based on the two-tailed Student's t-test. (**e**–**h**) Same as (a–d), but for the SH flux (Wm^{-2}). (**i**–**l**) Same as (**a**–**d**), but for the GH flux (Wm^{-2}). All fluxes are positive upward

Table 2 The mean planetary boundary layer height (in m) determined from each WRF simulation during each season and time of day averaged over the urban surface

	DJF Daytime	ASO Daytime	DJF Nighttime	ASO Nighttime
CTL	1182	1288	190	398
URB	1184	1288	205	413
CON	1180	1287	175	383
MOD	1177	1285	159	369
AGR	1174	1283	142	354

decreased LST and 2-m temperature difference (not shown). Despite the significance in AGR, these changes in SH are small in magnitude, which prevents significant changes in LST to occur downwind of the city. For the GH change patterns in DJF nighttime (Fig. 4i–l), the mean changes are about one-third of the mean changes in magnitude compared to DJF daytime. Since the GH flux at nighttime is positive, i.e., ground heat directed upward through a heat release, the sign of the change is reversed compared to daytime. The decrease in GH for the URB experiment during daytime indicates more heat retention (Fig. 2m) and thus more ground heat release at nighttime, i.e., an increase in the GH flux, and warmer LST. In contrast, GH decreases for the CON, MOD, and AGR experiments since there is less heat storage during the daytime for these experiments (Fig. 2b–c), which causes less heat release at nighttime and cooler LST. The influence of advection is not as noticeable for the GH flux. For the AGR simulation (Fig. 4l), there is a small area west of the city that experiences an increase in the GH flux. This may be due to the increased SH flux in the downwind area that has increased heat conduction and thus enabled more ground heat release at nighttime. Similar to the previous cases, despite the significant changes in SH and GH for the URB and CON experiments, no significant changes are shown for LST in these experiments. Significant changes in LST are only exhibited for MOD and AGR, in which the entire city exhibits significant grid-level changes.

Figure 5 shows the mean LST, SH and GH changes for ASO nighttime. The LST changes are of greater magnitude compared to ASO daytime but are less than in DJF nighttime. The LST response to a 10% change in urban fraction is not linear, similar to DJF nighttime. For CON, the mean urban LST decreased by 0.25°C, which then decreased by 0.29°C to a mean decrease of −20.54°C in MOD, and further

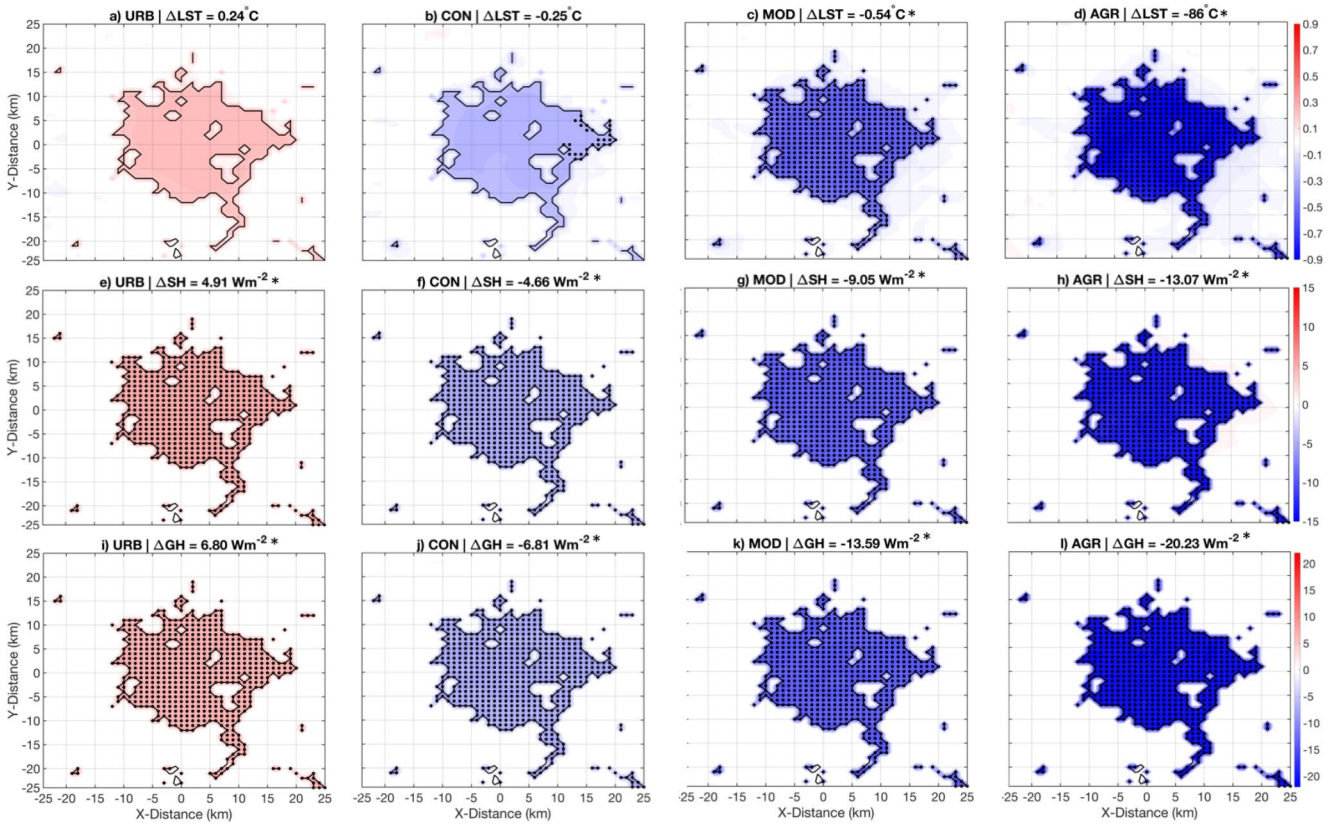

Fig. 5 Same as Fig. 4, but for ASO nighttime

decreased by 0.32ºC to a mean decrease of −20.86ºC in AGR. For URB, the mean LST increased by 0.24ºC. Also similar to DJF nighttime, a downwind effect is noticeable mainly for MOD and AGR. However, changes in LST are now to the east of the city since the mean simulated wind direction is from the west in ASO (not shown). Additionally, the downwind effect is weaker in ASO nighttime compared to DJF nighttime, likely due to the smaller LST response, which determines the downwind effect through advection. The smaller LST response in ASO nighttime is likely related to its deeper PBL compared to DJF nighttime (Table 2), as shallower boundary layers have been shown to influence LST more than deeper boundary layers (Davy et al. 2017). The SH and GH change patterns and magnitude are similar to DJF nighttime. Additionally, the downwind effect for SH is only evident in the MOD and AGR experiments, in which both show an insignificant increase in SH east of the city, again due to increased near-surface temperature gradients. The influence of advection on the GH flux is nonexistent. Finally, despite the significant mean changes in SH and GH throughout the city for all experiments, significant mean changes in LST mainly exist in the MOD and AGR experiments. A few grids are significant in the CON experiment.

3.2 Relationships between the changes in LST and LH, SH, and GH fluxes

Figure 6 shows the daytime relationship between the change in urban LST and the change in urban LH for all experiments relative to the CTL in DJF and ASO. For both seasons, each simulation shows a sharp urban LST decrease as urban LH increases and has a significant, negative temporal correlation coefficient ($r \sim -0.99$ for all simulations in DJF and $r \sim -0.98$ for all simulations in ASO). The slope values indicate that in all simulations in DJF, a daytime urban LH flux positive change would lead to a negative daytime urban LST change at a rate of about −0.03ºC per 1 Wm^{-2} since increased evaporation promotes surface cooling. The opposite is true for an urban LH flux decrease as in the URB simulation. In ASO, the rate of change for all simulations is about −0.022ºC per 1 Wm^{-2}. The rate of change in DJF is slightly higher than in ASO likely due to the shallower PBL simulated in DJF (Table 2), which would confine the responses to vegetation closer to the ground due to less vertical mixing. In addition, as the urban vegetation cover increases from URB to AGR, the seasonal-mean urban LH increases while the seasonal-mean urban LST decreases at a rate of −0.007ºC per 1 Wm^{-2} in DJF and −0.006ºC per

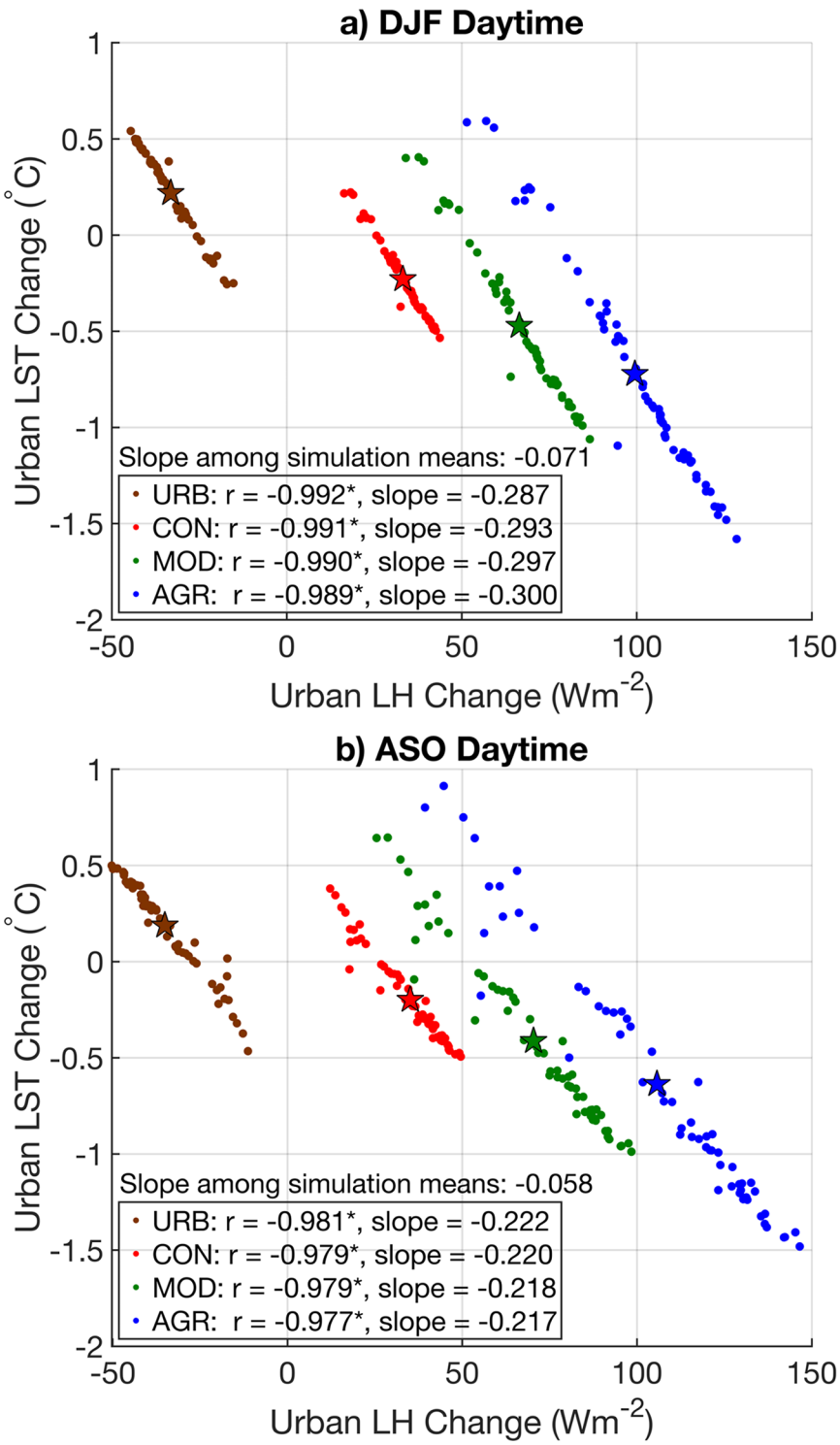

Fig. 6 (**a**) The 17 December 2017–14 February 2018 (DJF) daytime temporal relationship between the daily change in the urban LH flux (Wm^{-2}) and the daily change in urban LST (ºC) for the URB (brown), CON (red), MOD (green), and AGR (blue) simulations relative to the CTL daily value. (**b**) Same as (**a**), but for 17 August 2018–15 October 2018 (ASO) daytime. The temporal correlation coefficient (r) and slope (0.1ºC per 1 Wm^{-2}) are reported in the legend of each panel. An asterisk indicates the correlation coefficient is significant at the 10% level based on the two-tailed Student's t-test. The slope (0.1ºC per 1 Wm^{-2}) among the seasonal-mean urban LST and LH between the four simulations (denoted as stars) is also reported

1 Wm^{-2} ASO, which is weaker than the slope of the daily daytime changes for both seasons.

Figure 7 shows the relationship between the change in urban LST and the change in urban SH for all experiments during each season and time of day relative to the CTL. Figure 7a–b shows that in daytime, there is a direct relationship between changes in urban SH and urban LST with a slope of ~0.029ºC per 1 Wm^{-2} for all simulations in DJF and a slope of ~0.025ºC per 1 Wm^{-2} for all simulations in ASO. For each simulation in daytime, a significant temporal correlation is shown that is nearly perfectly linear (r~0.99 in DJF and ASO). The slopes and correlation coefficients indicate that a daytime urban SH flux negative change is associated with a daytime urban LST negative change since increased

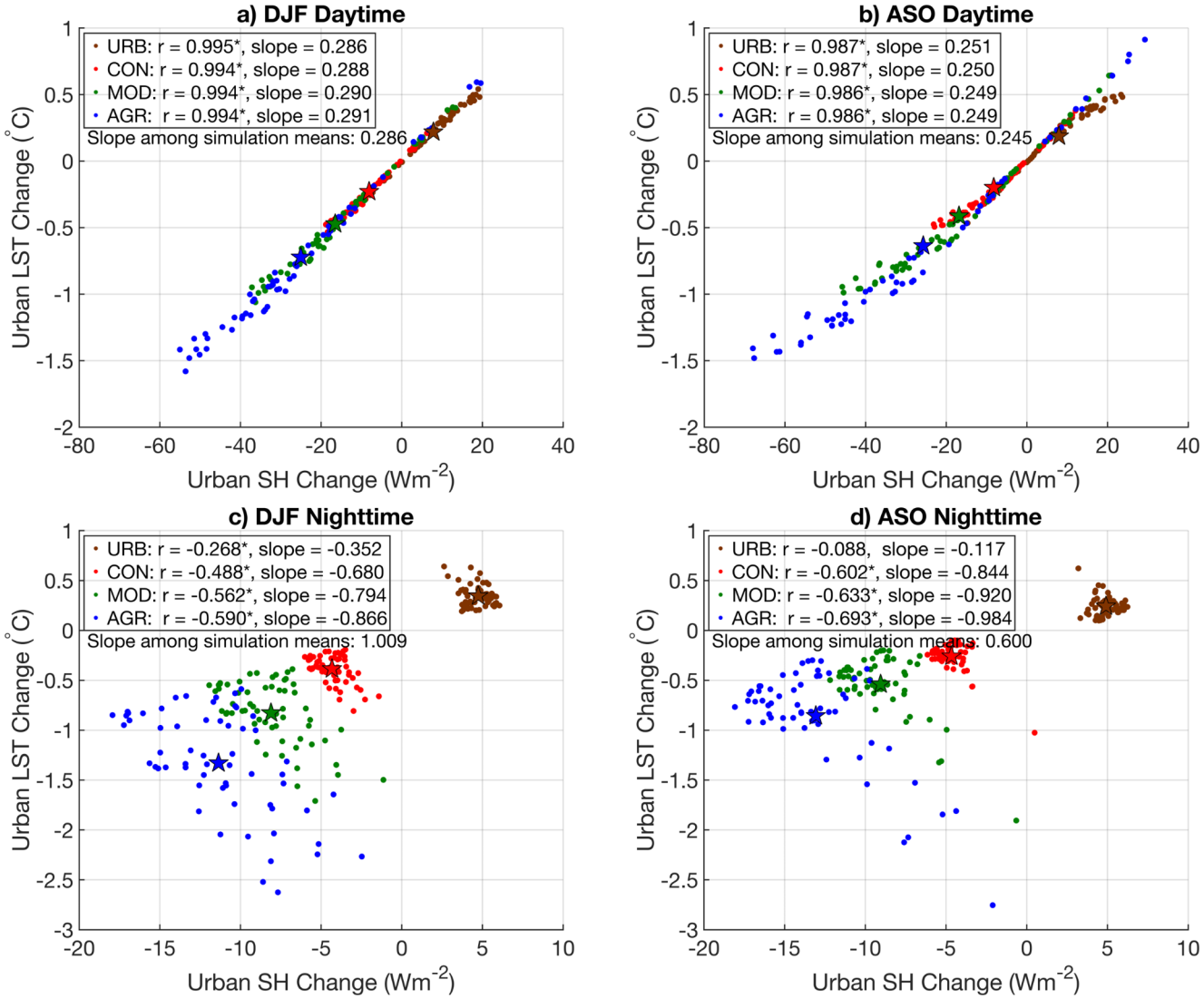

Fig. 7 (**a**) The 17 December 2017–14 February 2018 (DJF) daytime temporal relationship between the daily change in the urban SH flux (Wm^{-2}) and the daily change in urban LST (ºC) for the URB (brown), CON (red), MOD (green), and AGR (blue) simulations relative to the CTL run. (**b**) Same as (**a**), but for 17 August 2018–15 October 2018 (ASO) daytime. (**c**–**d**) Same as (**a**–**b**), but for nighttime. The temporal correlation coefficient (r) and slope (0.1ºC per 1 Wm^{-2}) are reported in the legend of each panel. An asterisk indicates the correlation coefficient is significant at the 10% level based on the two-tailed Student's t-test. The slope (0.1ºC per 1 Wm^{-2}) among the simulation-mean urban LST and SH (denoted as stars) is also reported

vegetation promotes more evaporative cooling, and thus less vertical heat transfer, and consequentially a lower LST. The opposite is true for an urban SH flux increase as in the URB simulation. Similar to Fig. 6, the rate of change is slightly higher in DJF likely due to the shallower PBL compared to ASO. The seasonal-mean urban LST increases as the seasonal-mean urban SH flux also increases at a rate of 0.029ºC per 1 Wm^{-2} in DJF, and again slightly less in ASO of 0.025ºC per 1 Wm^{-2} from AGR to URB, which is similar to the slopes of the daily daytime changes for each individual simulation for both seasons.

For the SH relationship at nighttime (Fig. 7c–d), all simulations in both seasons, except for the URB simulation in ASO, have a significant, negative temporal correlation that increases with a larger change in urban fraction. The nighttime correlations are weaker in magnitude than in daytime. The rate of change is not as consistent among the simulations compared to daytime as well. In DJF, the daily nighttime urban LST decreases at the fastest rate of −0.087ºC per 1 Wm^{-2} in AGR, which is followed by MOD (–0.079ºC per 1 Wm^{-2}), CON (–0.068ºC per 1 Wm^{-2}), and URB (–0.035ºC per 1 Wm^{-2}). Similarly, in ASO, the daily nighttime urban LST decreases with the fastest rate in AGR (–0.098ºC per 1 Wm^{-2}), followed by MOD (–0.092ºC per 1 Wm^{-2}), CON (–0.084ºC per 1 Wm^{-2}), and URB (–0.012ºC per 1 Wm^{-2}). The negative relationship suggests that an

increased nighttime urban SH flux change is associated with a decreased nighttime urban LST change relative to the CTL. During daytime the urban SH flux is positive; therefore, the flux is directed from the surface to the atmosphere. At nighttime, the urban SH flux is often negative, and thereby directed toward the surface since the surface becomes cooler than the lower atmosphere (i.e., nocturnal inversion) due to radiative cooling. Figure 7a–b show that the daytime seasonal-mean urban LST and SH decrease as the urban vegetation cover increases, which coincides with the daytime seasonal-mean LH increase and LST decrease from URB to AGR (Fig. 6). A lower daytime LST would also generally lead to a lower nighttime LST, and thus a larger downward SH flux at night, which helps to explain the seasonal-mean nighttime changes from AGR to URB shown in Fig. 7c–d that have a positive slope of 0.101ºC per 1 Wm^{-2} in DJF and 0.060ºC per 1 Wm^{-2} in ASO. However, a lower daily nighttime urban LST change tends to be associated with a smaller downward nighttime urban SH flux change among the simulations, which suggests that the nighttime urban LST and 2-m temperature difference becomes weaker as nighttime LST decreases for the experiments and becomes closer to equilibrium with 2-m temperature.

Figure 8 shows the relationship between the change in urban LST and the change in urban GH for all experiments during each season and time of day relative to the CTL. Figure 8a shows that in DJF daytime, a high urban GH flux change (i.e., decreased heat storage) is associated with a high urban LST change with a slope ranging from 0.107–0.151ºC per 1 Wm^{-2} and significant temporal correlation coefficients ranging from 0.53 to 0.74 from URB to AGR. Therefore, as the daily daytime urban GH flux becomes more positive, which is indicative of more

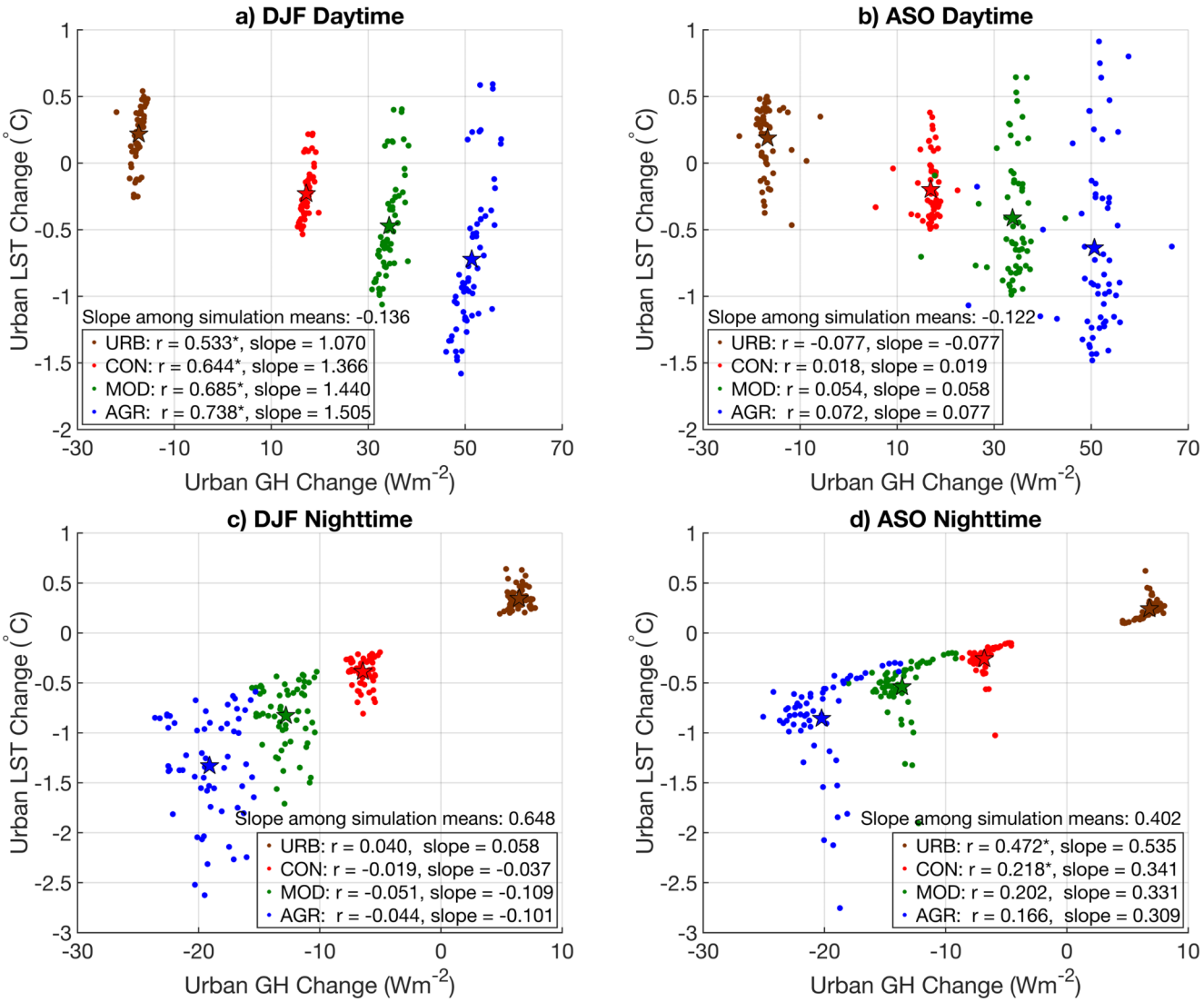

Fig. 8 Same as Fig. 7, but for the GH flux

ground heat storage release that would warm the surface, the daily daytime urban LST change also increases. Comparing the seasonal-means shows that as vegetation cover increases from URB to AGR in DJF daytime, the mean urban LST decreases as the mean urban GH flux increases at a rate of −0.136°C per 1 Wm^{-2}. Therefore, as vegetation increases, the mean urban LST decreases, and the mean urban GH increases as less heat is retained. For ASO daytime (Fig. 8b), none of the correlations are significant and the slopes are weak. The seasonal-mean slope is slightly less compared to DJF daytime (–0.122°C per 1 Wm^{-2}). For DJF nighttime (Fig. 8c), again the slopes are weak and none of the correlations are significant. The seasonal-mean slope of 0.648°C per 1 Wm^{-2} indicates that as vegetation decreases from AGR to URB, the mean urban GH flux increases (i.e., more nighttime heat release) and the mean urban LST also increases, which is likely due to low vegetation over the urban surface being able to retain more daytime heat, which then corresponds to a large heat release at nighttime. For ASO nighttime (Fig. 8d), the slopes are positive and the correlation coefficients are only significant for URB and CON, which indicates that as the urban GH flux increases and more heat is released, the urban LST also increases. The seasonal-mean slope is slightly less than in DJF nighttime of 0.402°C per 1 Wm^{-2} from AGR to URB.

3.3 Impact of vegetation on surface fluxes and UHI intensity

Figure 9 shows the relationship between urban fraction and mean UHI intensity for the CTL and perturbation experiments. As expected, UHI intensity increases linearly as urban fraction increases. For the AGR simulation, which represents the largest change in urban fraction (i.e., 30% decrease), the largest change in UHI intensity occurs in DJF nighttime of −0.66°C, followed by ASO nighttime of −0.42°C, DJF daytime of −0.35°C, and ASO daytime −0.31°C. The same ordering of the largest to smallest change in UHI intensity follows for the URB, CON, and MOD simulations as well. Thus, the nighttime UHI intensity appears to be the most sensitive to urban fraction change, especially during DJF. The high sensitivity of UHI intensity to vegetation cover during DJF nighttime is consistent with the largest urban LST change that was simulated during this time, which is again likely due to the shallow PBL that suppresses vertical mixing of the vegetation-induced surface changes (Table 2).

Using the linear line of best fit (Fig. 9), the urban fraction needed to obtain a neutral UHI of 0°C in DJF daytime is 0.85, which corresponds to a 5.56% decrease in urban fraction compared to the CTL. This is the only case in which solely decreasing impervious urban land and increasing pervious vegetation cover by a realistic amount as compared to the CTL could cancel the UHI in Bengaluru. In comparison, an urban fraction of 0.59 would be needed in ASO daytime, 0.16 in DJF nighttime, and 0.01 in ASO nighttime. These urban fractions represent a decrease of 34%, 82%, and 99% for ASO daytime, DJF nighttime, and ASO nighttime, respectively, compared to the CTL urban fraction of 0.90. These decreases in urban fraction are likely too high to be accomplished.

These results indicate that increasing vegetation alone will not cancel the UHI in Bengaluru. However, a 10% decrease in urban fraction, which could possibly be achieved, can certainly help Bengaluru reduce its extreme heat. In particular, Fig. 9c shows that the mean reduction in UHI intensity for 10% decrease in urban fraction in DJF nighttime is significant compared to the CTL. Reducing nighttime UHI intensity has been linked to a lower risk of heat-related illnesses for urban residents and can reduce energy demands when residents are in their homes (Frumkin 2002; Murage et al. 2017). This is especially important since DJF nighttime has the highest mean UHI intensity of 1.70°C based on the CTL mean values and has the highest sensitivity to urban fraction (Fig. 9).

4 Conclusions

To fill the gap in investigating UHI mitigation strategies over India, this study investigated the impacts of perturbed vegetation amount by various percentages over Bengaluru, India since vegetation amount is the leading driver of urban heat for the city (Sussman et al. 2021). This was achieved using WRF 1 km simulations by perturbing urban fraction by +10%, −10%, −20%, and −30% compared to its CTL value of 0.90 in each urban land cover grid, in which decreases represent more pervious, vegetated land cover. The responses in LST, the LH, SH and GH fluxes, and UHI intensity were examined. The strength of the relationships between the change in urban LST and changes in urban LH, SH, and GH were computed. It was also determined if the UHI could be cancelled through only decreasing urban fraction by a uniform amount throughout Bengaluru.

Results show that increases in vegetation lead to more upward LH flux during daytime and decreases in LST and SH during daytime and nighttime. During daytime, increased vegetation resulted in less downward GH flux, indicating less ground heat storage. This leads to less upward GH release, which cools the surface air, during nighttime as less heat is stored during the daytime under increased vegetation scenarios. These results occur since the GH flux is downward during daytime, and upward during nighttime. The results were opposite for a decrease in vegetation. The

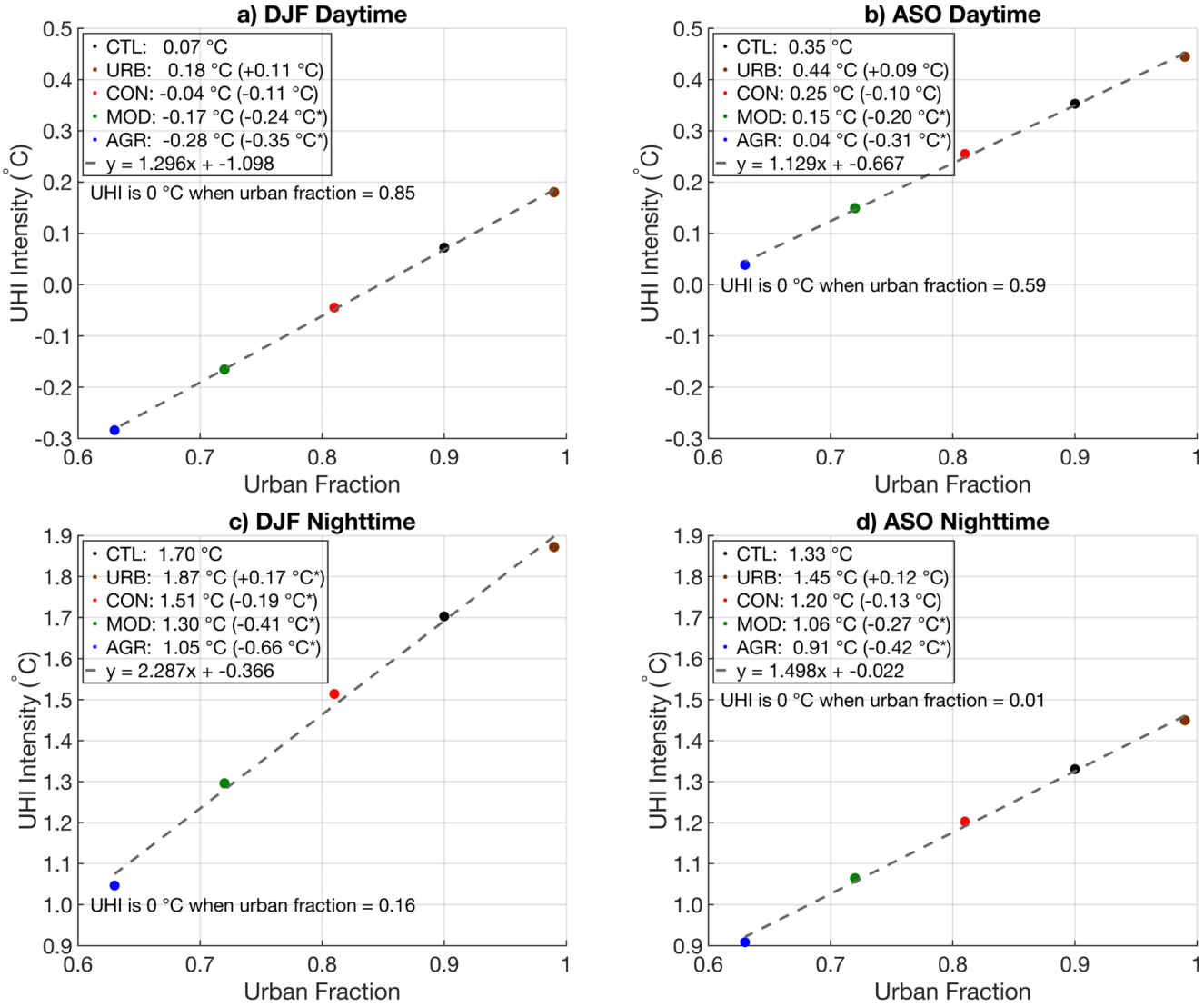

Fig. 9 (**a**) The 17 December 2017–14 February 2018 (DJF) daytime relationship between urban fraction and mean UHI intensity for the CTL (black), URB (brown), CON (red), MOD (green), and AGR (blue) simulations. The mean UHI intensity for each simulation is reported in the legend along with the associated mean change in UHI intensity with respect to the CTL simulation in parenthesis. An asterisk next to the mean change indicates that the mean difference is significant at the 10% level based on the two-tailed Student's t-test. The linear line of best fit is reported in the legend and was used to determine the urban fraction needed to produce a 0°C UHI intensity. (**b**) As in **a**), but for 17 August 2018–15 October 2018 (ASO) daytime. (**c**) As in (**a**), but for DJF nighttime. **d**) As in **a**), but for ASO nighttime

magnitude of the change in LST was higher during nighttime than daytime for both seasons.

The largest reductions in LST from increased vegetation occurred in DJF nighttime (simulation mean decrease of 0.44°C), which is likely a consequence of the shallowest PBL during this time (Table 2) that confines the vegetation-induced changes to the surface due to suppressed vertical mixing. For both seasons and both times of day, significant changes in LST were typically only observed when urban fraction was decreased by 20% or more (i.e., the MOD and AGR experiments) despite significant changes in the LH, SH, and GH fluxes for all simulations (Figs. 2, 3, 4 and 5). Therefore, large changes in LH, SH, and GH are needed to induce significant LST changes, even though changes in LH and SH are significantly correlated with changes in LST (Figs. 6 and 7). For all simulations in both seasons, the changes relative to the CTL in daily daytime urban LST were significantly negatively correlated with the changes in daytime urban LH since a higher LH flux is associated with a cooler LST due to more evaporative cooling (Fig. 6). For DJF and ASO daytime, the urban change in daily LST was significantly positively correlated with the urban change in daily SH since a low SH flux is associated with a low LST due to reduced surface-air temperature gradients, which is brought about by increased evaporative cooling (Fig. 7). During nighttime, the relationship between the urban

change in LST and urban change in SH is negative, albeit still significant (Fig. 7). The negative relationship arises due to the downward SH flux becoming weaker at nighttime as urban LST decreases and becomes closer in value to 2-m temperature, thus weakening the LST and 2-m temperature difference, which largely determines the magnitude of the SH flux. The relationship between the changes in the urban GH flux and urban LST was significant only during DJF daytime (Fig. 8). The relationships between the changes in urban LH and urban SH with urban LST were stronger due to nearly perfectly linear correlations compared to the relationship between the changes in urban GH and LST, which have weaker correlations. Therefore, changes to the LH and SH fluxes are likely the key drivers of the LST responses to vegetation modification.

Overall, it is unlikely the UHI of Bengaluru can be canceled via increasing vegetation alone (Fig. 9). However, a 10% decrease in urban fraction, which may be realistic, can lead to a substantial reduction in UHI intensity and thus could have significant benefits to public health and energy demands, especially during DJF nighttime when the CTL mean UHI intensity is highest (1.70°C) and a 10% decrease in urban fraction produces a statistically significant reduction (by 0.19°C) in UHI intensity (Fig. 9).These results suggest that the shallow PBL in DJF nighttime (Table 2) can significantly enhance the UHI and its sensitivity to vegetation cover. This may also explain why UHI intensity has a large sensitivity to urban fraction change in DJF nighttime (Fig. 9).

A limitation of this study is the absence of an urban morphology dataset, which can classify each urban grid based on its urbanization intensity, and thus better tune the urban fraction parameter for each urban grid and allow for heterogeneity in urban land cover throughout Bengaluru. As discussed in Sussman et al. (2024), these datasets are difficult to obtain for India. Therefore, the urban fraction values for the CTL experiment were based on the results of the MODIS EVI dataset over the city (Sussman et al. 2019) to obtain a baseline understanding of how WRF performs in simulating Bengaluru's UHI with homogeneous urban land cover. As urban morphology datasets continue to be advanced, future work should perform similar simulations using these data to better specify urban fraction, which may lead to improved simulations of surface fluxes and LST, and thus also improve the understanding of mechanisms and potential mitigation strategies. Another limitation of this study is that multiple years of the DJF and ASO seasons were not simulated, so a long-term climatology of LST and surface flux responses due to vegetation changes cannot be established. However, since 60 days within the DJF and ASO 2018 seasons were simulated and averaged, the results represent a robust daily response to the vegetation perturbations with most of the day-to-day noise being smoothed out. Including more years of simulations to determine the daily mean response to the vegetation forcing may involve different atmospheric background conditions, which may alter the results.

Future work can consider other mitigation strategies that are still based on the leading mechanism of urban heat in Bengaluru. For example, Sussman et al. (2019) showed that Bengaluru is expanding radially outward. Therefore, the most recently urbanized land on the outskirts of Bengaluru likely is not as urbanized as the city center. As a result, it may be more realistic to increase vegetation by a substantial amount in those areas. This would likely result in cooling of the outskirts and due to the downwind effect, temperature advection would aid in cooling central areas of the city. Future work can also investigate the impacts of combining mitigation strategies, such as increasing vegetation to promote evaporative cooling and increasing surface albedo to promote the reflection of solar radiation.

Future work should also investigate any potential regional impacts of increasing vegetation to reduce Bengaluru's UHI. For example, since increased vegetation increases the LH flux, this would increase available moisture and potentially increase the frequency, amount, and intensity of precipitation. Recently, Patel et al. (2021) investigated the impact of using green roofs to curb UHI intensity in Mumbai, India on precipitation amount. They simulated three cases in WRF for varying amounts of greenness and found accumulated rainfall to increase by a wide range of 1–72%. An increase in rainfall could lead to higher runoff and increase the risk of floods. Therefore, before any vegetation-based mitigation strategy is implemented in Bengaluru, future work should determine how the local climate could change and the associated implications of the change. These potential impacts to local climate due to UHI mitigation illustrates the complexity of developing and testing mitigation strategies.

Acknowledgements The authors would like to thank the Editor and two anonymous reviewers for their constructive feedback.

Author contributions HS conceptualized the study. HS performed the simulations and had initial discussions with AD and LZ. AD and LZ helped refine the methods. HS performed the calculations, made the figures, and wrote the first draft of this manuscript. AD and LZ helped revise this manuscript and provided feedback.

Funding The research effort of HS is supported by the Science, Mathematics, and Research for Transformation (SMART) fellowship from the Department of Defense. AD acknowledges funding support from the National Science Foundation (grant nos. AGS-2015780 and OISE-1743738). LZ acknowledges funding support from the National Science Foundation (AGS-1854486).

Data availability The MODIS Terra and Aqua combined land cover dataset is available from https://e4ftl01.cr.usgs.gov/MOTA/MCD12Q2.006/. The MODIS LST dataset is available from https://e4ftl01.cr.usgs.gov/MOLT/MOD11A2.006/ for Terra and https://e4ftl01.cr.usgs

.gov/MOLA/MYD11A2.006/ for Aqua. The ERA5 reanalysis data is available from https://cds.climate.copernicus.eu/cdsapp#!/dataset/reanalysis-era5-pressure-levels?tab=overview for pressure level data and https://cds.climate.copernicus.eu/cdsapp#!/dataset/reanalysis-era5-single-levels?tab=overview for surface data. The WRF model can be downloaded from https://www.mmm.ucar.edu/models/wrf. The simulations presented in this study can be made available by contacting Heather Sussman (Heather.S.Sussman@usace.army.mil).

Declarations

Competing interests The authors declare no competing interests.

References

Belward AS, Estes JE, Kilne KD (1999) The IGBP-DIS global 1-km land-cover data set DISCover: a project overvie. Photogramm Eng Remote Sensing 65:1013–1020

Beradi U, Jandaghian Z, Graham J (2020) Effects of greenery enhancements for the resilience to heat waves: a comparison of analysis performed through mesoscale (WRF) and microscale (Envi-met) modeling. Sci Total Environ 747:141300

Bougeault P, Lacarrerè P (1989) Parameterization of orography-induced turbulence in a mesobeta-scale model. Mon Weather Rev 117:1872–1890

Cady TJ, Rahn DA, Brunsell NA, Lyles W (2020) Conversion of abandoned property to green space as a strategy to mitigate the urban heat island investigated with numerical simulations. J Appl Meteorol Climatol 59:1827–1843

Chen F, Dudhia J (2001) Coupling an advanced land surface-hydrology model with the Penn State–NCAR MM5 modeling system. Part 1: model implementation and sensitivity. Mon Weather Rev 129:569–585

Chen F, Kusaka H, Bornstein R et al (2011) The integrated WRF/urban modelling system: development, evaluation, and applications to urban environmental problems. Int J Climatol 31:273–288. https://doi.org/10.1002/joc.2158

Davy R, Esau I, Chernokulsky A, Outten S, Zilitinkevich S (2017) Diurnal asymmetry to the observed global warming. Int J Climatol 37:79–93

Dudhia J (1989) Numerical study of convection observed during the Winter Monsoon experiment using a mesoscale two-dimensional model. J Atmos Sci 46:3077–3107

Filho WL, Icaza LE, Neht A, Klavins M, Morgan EA (2018) Coping with the impacts of urban heat islands. A literature based study on understanding urban heat vulnerability and the need for resilience in cities in a global climate change context. J Clean Prod 171:1140–1149

Frumkin H (2002) Urban sprawl and public heat. Public Health Rep 117:201–217

Grimm NB, Faeth SH, Golubiewski NE, Redman CL, Wu J, Bai X, Briggs JM (2008) Global change and the ecology of cities. Science 319:756–760

Hersbach H, Bell B, Berrisford P, Hirahara S, Horányi A, Muñoz-Sabater J, Nicolas J et al (2020) The ERA5 global reanalysis. Q J R Meteorol Soc 146:1999–2049

Imran HM, Kala J, Ng AWM, Muthukumaran S (2018) Effectiveness of green and cool roofs in mitigating urban heat island effects during a heatwave event in the city of Melbourne in Southeast Australia. J Clean Prod 197:393–405

Janjić ZI (1994) The step-mountain Eta coordinate model: further developments of the convection, viscous sublayer and turbulence closure schemes. Mon Weather Rev 122:927–945

Kim YH, Baik JJ (2002) Maximum urban heat island intensity in Seoul. J Appl Meteorol Climatol 41:651–659

Kishtawal CM, Niyogi D, Tewari M, Pielke RA, Shepherd JM (2010) Urbanization signature in the Observed heavy rainfall climatology over India. Int J Climatol 30, 1908–1916

Kusaka H, Kondo Y, Kikegawa Y, Kimura F (2001) A simple single-layer urban canopy model for atmospheric models: comparison with multi-layer and slab models. Bound -Layer Meteorol 101:329–358

Lenzhöler S, Van der Wulp NY (2010) Thermal experience and perception of the built environment in Dutch urban squares. J Urban Des 15:375–401

Li X-X, Norford LK (2016) Evaluation of cool roof and vegetations in mitigating urban heat island in a tropical city. Singap Urban Clim 16:59–74

Liu C, Ikeda K, Rasmussen R, Barlage M, Newman AJ, Prein AF, Chen F et al (2017) Continental-scale convection-permitting modeling of the current and future climate of North America. Clim Dyn 49:71–95

Lokoshchenko MA, Alekseeva LI (2023) Influence of meteorological parameters on the urban heat island in Moscow. Atmosphere 14:507

Mlawer EJ, Taubman SJ, Brown PD, Iacono MJ, Clough SA (1997) Radiative transfer for inhomogeneous atmospheres: RRTM, a validated correlated–k model for the longwave. J Geophys Res 102:16663–16682

Murage P, Hajat S, Kovats RS (2017) Effect of nighttime temperatures on cause and age-specific mortality in London. Environ Epidemiol 1, e005

Oke TR (1982) The energetic basis of the urban heat island. Q J R Meteorol Soc 108:1–24

Parthasarathy B (1984) Interannual and long-term variability of Indian summer monsoon rainfall. Proc Indian Acad Sci (earth Planet Sci) 93:371–385. https://doi.org/10.1007/BF02843255

Patel P, Karmakar S, Ghosh S, Aliaga DG, Niyogi D (2021) Impact of green roofs on heavy rainfall in tropical, coastal urban area. Environ Res Lett 16:074051

Ramachandran S, Kedia S, Srivastava R (2012) Aerosol optical depth trends over different regions of India. Atmos Environ 49:338–347

Skamarock WC, Klemp JB, Dudhia J, Gill DO, Liu Z, Berner J, Wang W, Powers JG, Duda MG, Barker DM, Huang W-Y (2019) A description of the advanced research WRF version 4. In: NCAR Technical Notes, p. 145. Retrieved from: https://opensky.ucar.edu/islandora/object/opensky%3A2898

Sudhira HS, Ramachandra TV, Subrahmanya B, M.H (2007) City profile: Bangalore. Cities 24:379–390

Sussman HS, Raghavendra A, Zhou L (2019) Impacts of increased urbanization on surface temperature, vegetation, and aerosols over Bengaluru, India. Remote Sens Appl : Soc Environ 16:100261

Sussman HS, Dai A, Roundy PE (2021) The controlling factors of urban heat in Bengaluru, India. Urban Clim 38:100881

Sussman HS, Dai A, Raghavendra A, Zhou L (2024) An evaluation of WRF urban canopy models over Bengaluru, Model. Earth Syst Environ 10:1783–1802

Taha H (1997) Urban climates and heat islands: albedo, evapotranspiration, and anthropogenic heat. Energ Build 25:99–103

Thompson G, Field PR, Rasmussen RM, Hall WD (2008) Explicit forecasts of winter precipitation using an improved bulk microphysics scheme. Part II: implementation of a new snow parameterization. Mon Weather Rev 136:5095–5115

United Nations (2018) World Urbanization Prospects – 2018 Revision. https://population.un.org/wup/. (accessed 29 April 2019)

Veena K, Parammasivam KM, Venkatesh TN (2020) Urban heat island studies: current status in India and a comparison with the international studies. J Earth Syst Sci 129:1–15

Xu D, Wang Y, Zhou D, Wang Y, Zhang Q, Yang Y (2024) Influences of urban spatial factors on surface urban heat island effect and its spatial heterogeneity: a case study of Xi'an. Build Environ 248:111072

Zhou J, Chen Y, Wang J, Zhan W (2011) Maximum nighttime urban heat island (UHI) intensity simulation by integrating remotely sensed data and meteorological observations. IEEE J Sel Top Appl Earth Observ Remote Sens 4:138–146